

See discussions, stats, and author profiles for this publication at: <https://www.researchgate.net/publication/228866743>

# Triboelectric Charging of Granular Insulator Mixtures Due Solely to Particle– Particle Interactions

ARTICLE *in* INDUSTRIAL & ENGINEERING CHEMISTRY RESEARCH · MARCH 2009

Impact Factor: 2.59 · DOI: 10.1021/ie8004786

---

CITATIONS

26

---

READS

103

3 AUTHORS, INCLUDING:



Keith M Forward

California State Polytechnic University, Po...

10 PUBLICATIONS 193 CITATIONS

SEE PROFILE

Article

## **Triboelectric Charging of Granular Insulator Mixtures Due Solely to Particle#Particle Interactions**

Keith M. Forward, Daniel J. Lacks, and R. Mohan Sankaran

*Ind. Eng. Chem. Res.*, **2009**, 48 (5), 2309-2314 • DOI: 10.1021/ie8004786 • Publication Date (Web): 29 July 2008

Downloaded from <http://pubs.acs.org> on May 16, 2009

### **More About This Article**

Additional resources and features associated with this article are available within the HTML version:

- Supporting Information
- Access to high resolution figures
- Links to articles and content related to this article
- Copyright permission to reproduce figures and/or text from this article

[View the Full Text HTML](#)



**ACS Publications**  
High quality. High impact.

# Triboelectric Charging of Granular Insulator Mixtures Due Solely to Particle–Particle Interactions

Keith M. Forward, Daniel J. Lacks,\* and R. Mohan Sankaran

Department of Chemical Engineering, Case Western Reserve University, Cleveland, Ohio 44106

Triboelectric charging is widely observed in granular systems, but the physics underlying the phenomenon is not well understood. A critical challenge for experimental studies of triboelectric charging is to obtain reproducible data that can be linked to theoretical predictions. Toward this end, we develop and perform experiments on the triboelectric charging of granular mixtures with varying composition. A benchtop particle flow apparatus has been constructed that operates under low vacuum (70 Torr); performing experiments in a clean and controlled environment reduces the effects on charging caused by contaminants, humidity, etc. The apparatus is designed such that only particle–particle interactions occur (i.e., no particle–wall interactions). A noncontact method of measuring charge is employed to limit probe–particle charging (or discharging). Both time-dependent and steady-state behaviors are investigated. Various granular insulator materials are studied to investigate the effect of system composition on the triboelectric charging. In all cases, the binary mixtures produce much greater triboelectric charging than the single-component systems.

## Introduction

The triboelectric charging of granular systems is poorly understood even though it has important consequences, as pointed out recently in both industrial<sup>1</sup> and natural contexts.<sup>2</sup> Triboelectric charging is a process that occurs when two initially neutral surfaces come into contact, transfer charge, and remain charged with the opposite polarity when they are separated. The polarity is determined by the material properties (in a way that is not understood), as described empirically by the triboelectric series;<sup>3</sup> the charging process is currently so poorly understood that it is not even clear whether it is the transfer of electrons or ions that causes the charging.<sup>4,5</sup>

A wide range of consequences of triboelectric charging of granular materials arise in both industry and nature. In industry, intentional triboelectric charging forms the basis of many processes in the imaging industry,<sup>1</sup> but unintentional triboelectric charging can cause problems in other processes. In fluidized bed reactors and pneumatic transport systems, triboelectric charging disrupts the desired flow patterns and can lead to problems such as the formation of polymer sheets in polymerization reactors<sup>6</sup> and nonuniform dosages in pharmaceutical products.<sup>7</sup> For pharmaceuticals used in powder form (e.g., with dry powder inhalers), triboelectric charging during dispersal can alter the drug delivery.<sup>8</sup> In nature, lightning is caused by the charging of dust and ice particles, which produce large potentials leading to electrical breakdown.<sup>9</sup> Similarly, volcanic lightning occurs when the ash particles in volcanic plumes triboelectrically charge, producing large electric fields sufficient for gas breakdown.<sup>10</sup> The triboelectric charging of sand or dirt in dust devils generates bipolar electric fields with potentials of several thousand kilovolts, which have the potential of damaging electronic equipment.<sup>11</sup>

The present study addresses the triboelectric charging of granular mixtures arising specifically from particle–particle interactions and relates the composition of the mixture to the magnitude of charging. In general, particles can charge from interactions with either the container wall (or its associated components) or other particles; the relative importance of these

two contributions depends on the situation. In sand storms and dust devils, the particles seldom pick up charge from different materials at boundaries. In fluidized beds and pneumatic transport through pipes, the relative importance of these two factors will likely depend on the surface-to-volume ratio of the container as well as the properties of the materials involved; for example, in large silos or reactors, only a small proportion of the material is in contact with the walls.

While previous studies have elucidated the factors affecting electrostatic charging in single-component granular systems,<sup>12–31</sup> to the best of our knowledge, the composition dependence of triboelectric charging of granular mixtures arising only from particle–particle interactions has not been examined. The composition dependence of charging in granular mixtures has also been examined, in regard to electrostatic separations and pharmaceutical systems, but the charging behavior was unclear due to interaction of the particles with both other particles and the container walls.<sup>32–35</sup> Other studies examined the charging of particles in contact with larger beads of a different composition, in analogy with the toner charging process.<sup>36–39</sup> We are aware of one work that aimed to restrict charging to interactions only between particles (in single-component systems), by lining the walls of the container with sheets of the same material being studied;<sup>40</sup> however, while ostensibly the same material, the sheets and particles may have somewhat different compositions (e.g., due to different processing methods).

**Experimental Setup.** We have developed a methodology to determine the triboelectric charging of granular mixtures as a result of particle–particle interactions. To do this, our apparatus creates particle flow in which the moving particles only come in contact with other particles, and we measure the electrostatic charging with a probe that does not contact the particles. Additionally, to eliminate particle charging from size variations, each particle sample is sieved to keep similar particle sizes for each material (note that previous work has shown that the particle size distribution can have significant effects on triboelectric charging<sup>14–18,30,37</sup>). To improve the reproducibility, the experiments are carried in a controlled (low-vacuum) environment. In addition, we attempt to decouple the charging behavior from flow effects (which are functions of particle

\* To whom correspondence should be addressed. Phone: (216) 368-4238. E-mail: daniel.lacks@case.edu.

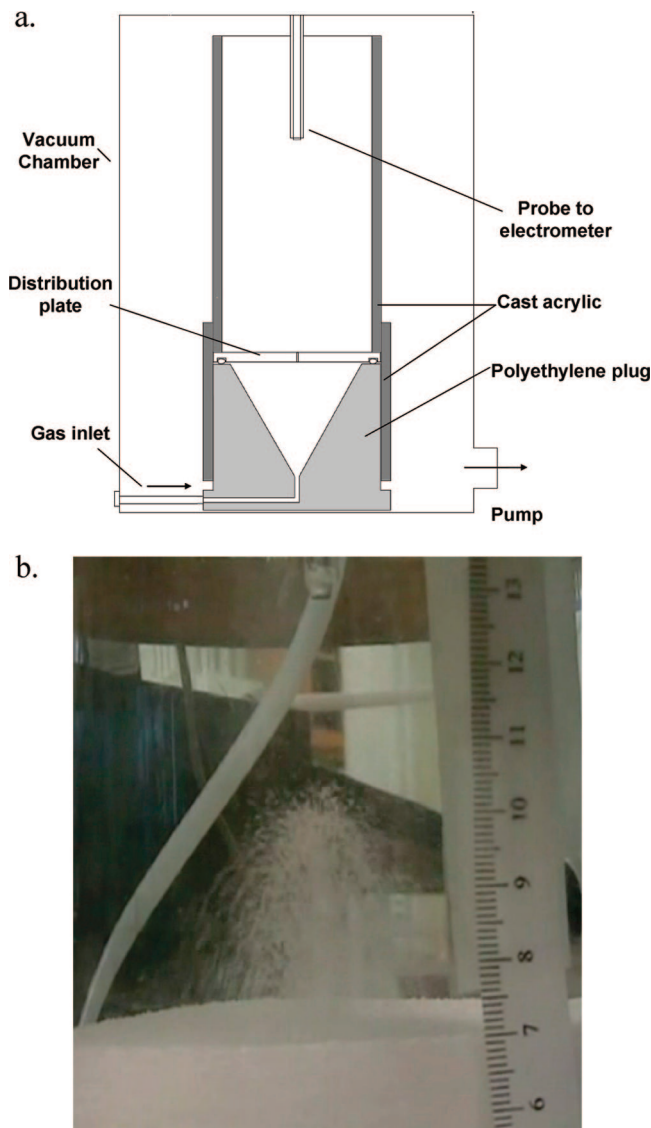


**Figure 1.** (a) Schematic of the particle flow apparatus. (b) Image of the fountain-like flow that arises from a single-hole distribution plate.

density and size, bed height, etc.) by running all experiments with the same bed height and very similar particle sizes and examining how charging occurs over a range of different pressure drops rather than at individual pressure drops.

**Particle Flow Apparatus.** As schematically shown in Figure 1, a particle bed reactor was constructed from cast acrylic tubing and polyethylene. An acrylic tube 7 in. long with a 4-in. inner diameter was fixed inside a tube with a 4.5-in. inner diameter. A high-density polyethylene rod was then machined to fit snugly into the bottom of the two-piece acrylic reactor. To evenly distribute the gas flow to the bed, the polyethylene was machined with a conical cavity. A channel was machined from the bottom of the cone to the side of the polyethylene plug to connect the gas flow. A distribution plate was machined from 1/4-in.-thick cast acrylic and sealed with an O-ring between the polyethylene plug and the acrylic. A single-hole distribution plate with a diameter of 500  $\mu\text{m}$  was employed to ensure controlled flow of particles as compared to a more conventional multihole configuration: the single-hole configuration generates “fountain-like” flow in which the stream of particles does not come into contact with the walls of the reactor. With this type of flow, the particles in contact with the distribution plate and the side walls are stagnant since only particles above the hole

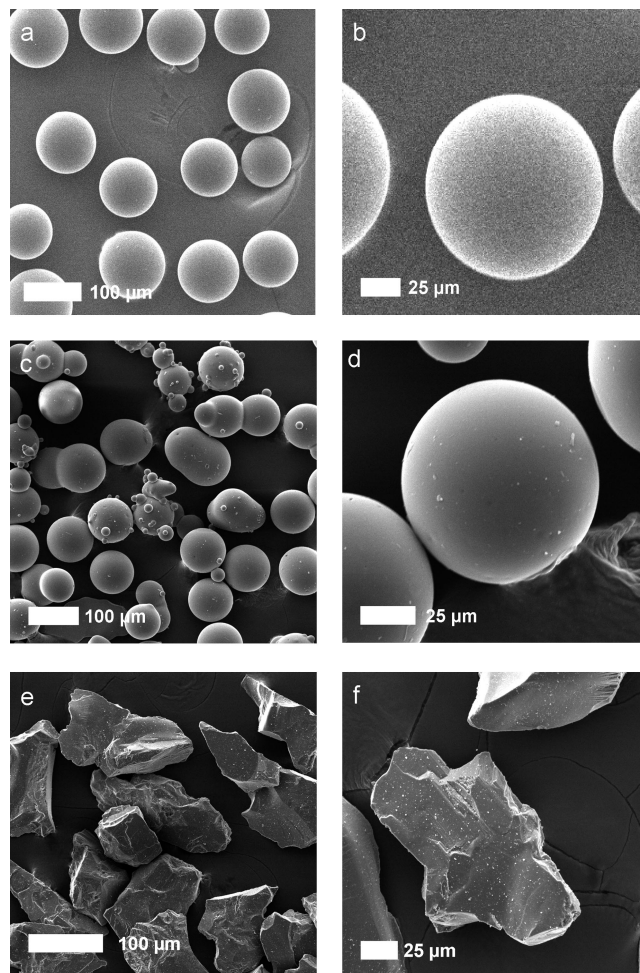


**Figure 2.** Scanning electron microscope images of (a,b) acrylic particles, (c,d) soda lime glass particles, and (e,f) aluminum oxide particles.

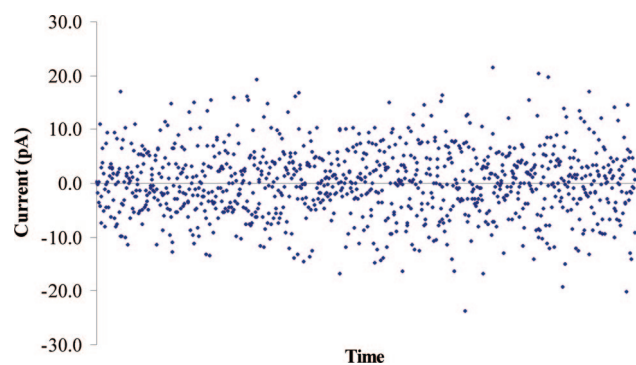


**Figure 3.** Example of the raw current data measured by the electrometer as a function of time. The time axis extends over 1 min (1000 data points).

of the distribution plate are involved in the flow. As a result, only particle–particle contact is caused by the flow (see Figure 1b). Furthermore, the particle flow is aligned with the electrostatic probe to measure particle charge directly.

An electrostatic probe, made from a 1/8-in.-diameter stainless steel rod shielded with quartz glass, was used to measure particle charging. The probe was connected to a Keithley 6517A electrometer, which measures the current drawn from the bed at intervals of  $\sim 60$  ms. The currents measured by the probe are induced by the charged particles that move in the vicinity of the probe. To minimize particle–probe interaction, the bottom of the probe was positioned  $\sim 10$  cm above the settled bed.



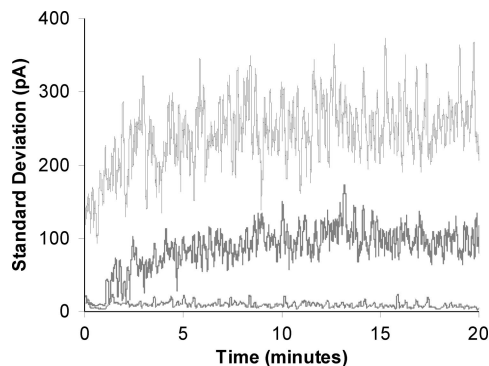


**Figure 4.** Results for the standard deviation of the current obtained for 100 data points (6-s intervals). Results are for the 75–25% aluminum oxide–acrylic mixture. The three curves, from bottom to top, represent results for pressure drops of 7.5, 9.2, and 10.1 Torr.

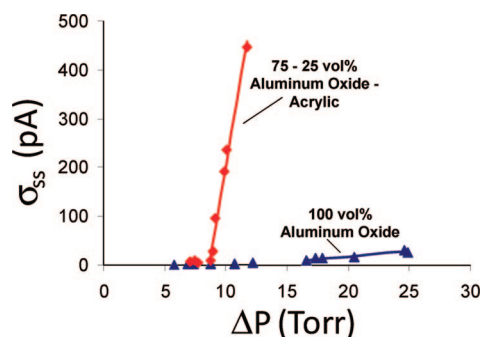


**Figure 5.** Steady-state standard deviations of the current,  $\sigma_{ss}$ , as a function pressure drop,  $\Delta P$ . Diamonds are results for the 75–25% aluminum oxide–acrylic mixture, and triangles are results for pure aluminum oxide. The results at higher pressure drops are fitted to a line, with slopes  $d\sigma_{ss}/d\Delta P = 136.4 \pm 10.2$  pA/Torr for the mixture and  $d\sigma_{ss}/d\Delta P = 1.9 \pm 0.2$  pA/Torr for the pure aluminum oxide.

The particle flow apparatus was placed in a cylindrical vacuum chamber (Laco Technology, Inc.) and enclosed by a Faraday cage to prevent interference from external electric fields. The vacuum chamber ensures a clean environment and minimizes the effects of impurities and humidity that can influence the charging behavior. An Edwards E2M1.5 vacuum pump was used to maintain a reduced pressure environment of 70 Torr. Two pressure transducers were used to measure the pressures in the vacuum chamber and of the inlet gas flow, respectively; the difference in pressure was used to determine the pressure drop across the fluidized bed. The chamber pressure and inlet gas flow rate were regulated by mass flow controllers.

**Granular Mixtures.** The triboelectric charging of binary mixtures composed of three different granular materials is investigated. Soda lime glass, aluminum oxide, and poly(methyl methacrylate) (acrylic glass) are used for this study. Granular materials with similar sizes are used in order to have similar fluidization characteristics and prevent particle size effects on charging behavior. Acrylic powder was obtained from Alfa Aesar with particle diameters of 70–85  $\mu\text{m}$ . Soda lime glass (Dragonite, Jayco Inc.) and aluminum oxide (Duralum) powders were obtained in bulk samples with large size distributions; these materials were sieved to obtain particles with diameters of  $\sim 90$ – $106$   $\mu\text{m}$  (170–140 mesh number). Scanning electron microscope images shown in Figure 2 confirm the size distribution and morphology of the particles. The compositions of the mixtures are given below in percent by volume.

**Experimental Procedure.** The height of the settled bed was maintained at 34 mm (330 mL) for each material. Since the various particle materials are similarly sized, the number of

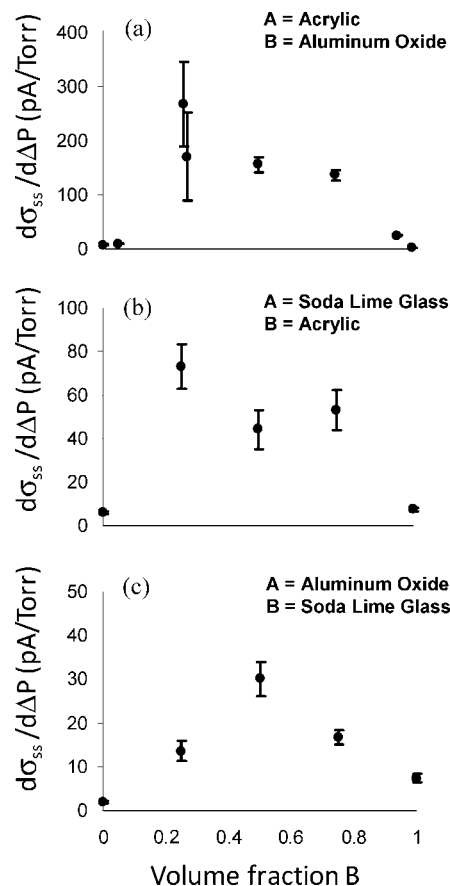


**Figure 6.** Results for the change in the steady-state standard deviation of the current with change in pressure drop ( $d\sigma_{ss}/d\Delta P$ ), for the (a) acrylic–aluminum oxide system, (b) soda lime glass–acrylic system, and (c) aluminum oxide–soda lime glass system.

particles in the bed was essentially constant. Before particles were placed in the bed, they were neutralized with an ion gun (Exair Inc.). The bed was then placed in the vacuum chamber and connected to the inlet gas flow of high-purity nitrogen gas. The chamber was evacuated to 20 Torr and purged with nitrogen gas to remove water vapor and air. The electrometer current, chamber pressure, and pressure drop were continuously measured over a period of 50 min. To perform experiments, the pressure was controlled at 70 Torr with flow rates in the range of 0.15–0.5 L/min; this pressure was chosen so that a low-pressure environment could be maintained while allowing for a wide range of flow rates. It should be noted that the flow rates required for fluidization under reduced pressure are much lower than those required at atmospheric pressure.

## Results

An example of raw current data from an experiment is shown in Figure 3. A positively charged particle will induce a positive current when moving toward the probe and a negative current when moving away from the probe; thus, while the instantaneous currents produced by this particle are non zero, the average current is zero. Each data point represents the total current induced from all charged particles moving near the probe. The fluctuations in the raw data occur because of changes in the number of particles near the probe, the magnitude and sign of the charge on each particle, and the direction each particle is moving with respect to the probe. If the particles do not touch

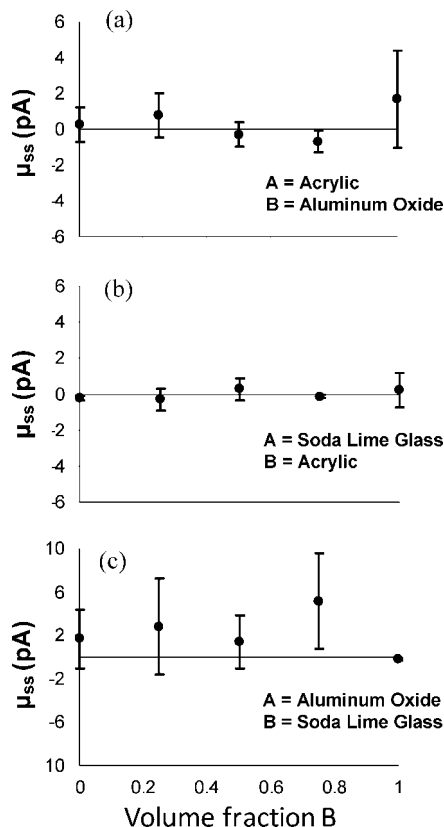


**Figure 7.** Results for the mean value of the current ( $\mu_{ss}$ ) (obtained as the mean overruns at all pressure drops) for the (a) acrylic–aluminum oxide system, (b) soda lime glass–acrylic system, and (c) aluminum oxide–soda lime glass system.

the probe (and transfer their charge to the probe), the mean current will equal zero since the contribution from each particle as it approaches the probe will be canceled by the contribution when it moves away from the probe. The magnitude of triboelectric charging observed in Figure 3 can be quantified by the standard deviation of the current measurements.

To address the transient behavior of charging, we track the time dependence of the standard deviation of the current over a short duration. In Figure 4, the results are shown for the standard deviation of the current calculated over 100 data points (total time, 6 s). Results are shown for three different flow rates. For the lowest flow rate, no charging is measured (for reasons discussed below). However, at the higher flow rates, a time-dependent response is clearly observed. Initially, the value of the standard deviation is low, which indicates little charge on the particles (note that the method of using 100 data points to determine a standard deviation prevents accurate results at very short times). As time increases, the value of the standard deviation increases, and it eventually reaches a steady-state value (denoted  $\sigma_{ss}$ ). The time scale for the charging to reach the steady-state value is  $\sim 5$ – $10$  min, which is similar to the time scales found for the triboelectric charging of fluidized beds.<sup>28,29</sup> This time dependence, which is similar in all systems, suggests that the steady-state results are due to charging rather than flow behavior in the bed (i.e., the flow behavior reaches steady state much more quickly).

The dependences of  $\sigma_{ss}$  on the imposed pressure drop are shown in Figure 5. The value of  $\sigma_{ss}$  is determined here as the standard deviation for the last 20 000 data points (i.e., when the charging in bed has reached equilibrium). For low flow rates (low pressure drop), the particles do not have sufficient velocity to be detected by the probe. However, at higher flow rates, the

value of  $\sigma_{ss}$  increases essentially linearly with the pressure drop. This increase occurs because, as the flow rate increases, the particles come closer to the probe and the number of particles sensed by the probe increases. As a way to decouple these flow effects from the charging behavior, the slope  $d\sigma_{ss}/d\Delta P$  is used to characterize the charging tendency of the granular system; we believe that this quantity will be relatively independent of the flow characteristics. As shown in Figure 5, the charging is much greater for the acrylic–aluminum oxide mixture than for the pure aluminum oxide system; this difference is quantified by the much larger value of  $d\sigma_{ss}/d\Delta P$  for the acrylic–aluminum oxide mixture.

The charging behaviors of the granular mixtures are assessed as a function of the composition of the mixtures. Figure 6 shows the results for  $d\sigma_{ss}/d\Delta P$  as a function of composition for the three binary systems examined (acrylic–aluminum oxide, soda lime glass–acrylic, and aluminum oxide–soda lime glass). For all three systems, the mixtures charge much more than the pure components (i.e., have much larger values of  $d\sigma_{ss}/d\Delta P$ ); in the case of the acrylic–aluminum oxide system, the charging of the mixture is more than 20-fold greater than the charging of the pure components. Also, the acrylic–aluminum oxide system charges significantly more than the other two systems.

The mean currents at steady state,  $\mu_{ss}$ , are also examined. As discussed above, the mean current will equal zero if the particles do not touch the probe. The observed mean currents are on the order of  $\sim 0.1$  pA, which is negligible compared to the instantaneous currents that fluctuate on the order of 10–1000 pA. Figure 7 shows that the dependence of the mean currents for all mixtures are zero within experimental error. Thus, it is concluded that the particles do not physically contact the probe and transfer charge to a significant extent.

## Discussion

The experimental approach described allows the measurement of triboelectric charging of granular materials solely from particle–particle interactions by using a flow apparatus that eliminates wall effects. The charging is measured with a contactless method to avoid particle charging (or discharging) through contact with the probe; the charging is then studied as a function of time since charge is never removed from the bed. The experiments are carried out in a low-vacuum environment to minimize the effects of humidity, dust, and other contaminants.

The difference in the charging of single-component systems as compared to binary mixtures is clearly illustrated in Figure 6: the binary mixtures charge much more than the single-component systems. This result is understandable theoretically since charge transfer during contact between surfaces would be expected to be driven by differences in the surface properties. For metals, the property that governs the charge transfer is the work function (i.e., the energy needed to remove an electron from the metal surface); electrons will be transferred from the metal with the lower work function to the metal with the higher work function, and the driving force for this charge transfer will increase with the relative difference in work function. For insulators, the situation is more complicated and not well understood, and an empirical “triboelectric series”, which orders materials by their propensity to gain positive charge triboelectrically, is used to determine the direction of charging.

The magnitude of charging for the three mixtures studied was found to be in the following order (from most charging to least

charging): (1) acrylic–aluminum oxide, (2) soda lime glass–acrylic, and (3) aluminum oxide–soda lime glass. It is understandable that the aluminum oxide–soda lime glass system would charge the least, because these materials are both oxides and thus would likely have somewhat similar surface properties. Regarding the charging of the two oxides with acrylic, the triboelectric series usually places silica glass further from acrylic than aluminum (we assume that studies on aluminum surfaces really address oxidized surfaces); thus, the triboelectric series would suggest the soda lime glass–acrylic mixture would charge more than the acrylic–aluminum oxide mixture, in contrast to what we observe. Various factors can lead to this difference. For example, the position of a material in a triboelectric series is not invariant but can depend on the surface texture, the details of the contact, the presence of contaminants, and temperature (which may affect the presence of contaminants).<sup>41</sup> Also, quantitative comparisons of different systems are complicated by differences in fluidization. Since the density, shape, and size distribution of the particles are different for each material, the fluidization behavior is somewhat different in all cases. For example, aluminum oxide is the densest of the materials and the most irregularly shaped, and higher flow rates were required to fluidize this material (see Figure 5). Thus, there is some inherent error in comparing the values of  $d\sigma_{ss}/d\Delta P$  for different systems because of differences in the nature of fluidization.

## Conclusion

We present the first experiments that address the composition dependence of the triboelectric charging of granular mixtures arising only from the interparticle interactions. The results show that the amount of charging in the binary mixtures is much greater than in single-component systems, which is in agreement with theoretical ideas regarding triboelectric charging.

## Acknowledgment

This project was funded by the Dow Chemical Company.

**Note Added after ASAP Publication:** The version of this paper that was published on the Web July 29, 2008 had an error in the author list of ref 38. The corrected version of this paper was reposted to the Web August 15, 2008.

## Literature Cited

- (1) Schien, L. B. Recent Progress and Continuing Puzzles in Electrostatics. *Science* **2007**, *316*, 1572–1573.
- (2) Shinbrot, T.; Herrmann, H. J. Static in motion. *Nature* **2008**, *451*, 773–774.
- (3) Shaw, P. E. Experiments on Tribo-Electricity. I. The Tribo-Electric Series. *Proc. R. Soc., A* **1917**, *94*, 16–33.
- (4) McCarty, L. S.; Whitesides, G. M. Electrostatic Charging Due to Separation of Ions at Interfaces: Contact Electrification of Ionic Electrets. *Angew. Chem., Int. Ed.* **2008**, *47*, 2188–2207.
- (5) Liu, C.; Bard, A. J. Electrostatic electrochemistry at insulators Nat. Mater. Advance online publication.
- (6) Stainforth, J. N. The Importance of Electrostatic Measurements in Aerosol Formulation and Reformulation. *Respir. Drug Delivery* **1994**, *4*, 303–311.
- (7) Hendrickson, G. Electrostatics and gas phase fluidized bed polymerization reactorwall sheeting. *Chem. Eng. Sci.* **2006**, *61*, 1041–1064.
- (8) Center for Drug Evaluation and Research. Guidance for Industry: MDI and DPI Products, Chemistry, Manufacturing and Control Documentation. 1998.
- (9) Stow, C. D. Atmospheric electricity. *Rep. Prog. Phys.* **1969**, *32*, 2–67.
- (10) Mather, T. A.; Harrison, R. G., Electrification of volcanic plumes, *Surv. Geophys.*, DOI 10.1007/s10712-006-9007-2.
- (11) Farrell, W. M.; Smith, P. H.; Delory, G. T.; Hillard, G. B.; Marshall, J. R.; Catling, D.; Hecht, M.; Traff, D. M.; Renno, N.; Desch, M. D.; Cummer, S. A.; Houser, J. G.; Johnson, B. Electric and Magnetic Signatures of Dust Devils from 2000–2001 MATADOR desert test. *J. Geophys. Res.* **2004**, *109*, E03004.
- (12) Guardiola, J.; Rojo, V.; Guadalupe, R. Influence of Particle, Fluidization Velocity and Relative Humidity on Fluidized Bed Electrostatics. *J. Electrostat.* **1996**, *37*, 1–20.
- (13) Liang, S.-C.; Zhang, J.-P.; Fan, L.-S. Electrostatic Characteristics of Hydrated Lime Powder during Transport. *Ind. Eng. Chem. Res.* **1996**, *35*, 2748–2755.
- (14) Ali, F. S.; Ali, M. A.; Ali, R. A.; Inculet, I. I. Minority charge separation in falling particles with bipolar charge. *J. Electrostat.* **1998**, *45*, 139–155.
- (15) Zhao, H.; Castle, G. P.; Inculet, I. I.; Bailey, A. G. Bipolar Charging of Poly-Disperse Polymer Powders in Fluidized Beds. *IEEE Trans. Ind. Appl.* **2003**, *39*, 612–618.
- (16) Zhao, H.; Castle, G. S. P.; Inculet, I. I. The Measurement of Bipolar Charge in Polydisperse Powder Using a Vertical Array of Faraday Pail Sensors. *J. Electrostat.* **2002**, *55*, 261–278.
- (17) Inculet, I. I.; Castle, G. S. P.; Aartsen, G. Generation of bipolar electric fields during industrial handling of powders. *Chem. Eng. Sci.* **2006**, *61*, 2249–2253.
- (18) Ali, F. S.; Inculet, I. I.; Tedoldi, A. Charging of polymer powder inside a metallic fluidized bed. *J. Electrostat.* **1999**, *45*, 199–211.
- (19) Matsusaka, S.; Oki, M.; Masuda, H. Bipolar charge distribution of a mixture of particles with different electrostatic characteristics in gas-solids pipe flow. *Powder Technol.* **2003**, *135*, 150–155.
- (20) Nomura, T.; Satoh, T.; Masuda, H. The environment humidity effect on the tribo-charge of powder. *Powder Technol.* **2003**, *135*, 43–49.
- (21) Yao, J.; Zhang, Y.; Wang, C.-H.; Matsusaka, S.; Masuda, H. Electrostatics of the Granular Flow in a Pneumatic Conveying System. *Ind. Eng. Chem. Res.* **2004**, *43*, 7181–7199.
- (22) Zhu, K.; Rao, S. M.; Huang, Q. H.; Wang, C.-H.; Matsusaka, S.; Masuda, H. On the electrostatics of pneumatic conveying of granular materials using electrical capacitance tomography. *Chem. Eng. Sci.* **2004**, *59*, 3201–3213.
- (23) Yao, L.; Bi, H. T.; Park, A.-H. Characterization of electrostatic charges in freely bubbling fluidized beds with dielectric particles. *J. Electrostat.* **2002**, *56*, 183–197.
- (24) Mehrani, P.; Bi, H. T.; Grace, J. R. Electrostatic charge generation in gas-solid fluidized beds. *J. Electrostat.* **2005**, *63*, 165–173.
- (25) Mehrani, P.; Bi, H. T.; Grace, J. R. Bench-scale tests to determine mechanisms of charge generation due to particle-particle and particle-wall contact in binary systems of fine and coarse particles. *Powder Technol.* **2007**, *173*, 73–81.
- (26) Mountain, J. R.; Mazumder, M. K.; Sims, R. A.; Wankum, D. L.; Chasser, T.; Pettit, P. H., Jr. Triboelectric Charging of Polymer Powders in Fluidization and Transport Processes. *IEEE Trans. Ind. Appl.* **2001**, *37*, 778–784.
- (27) Sickafoose, A. A.; Colwell, J. E.; Horanyi, M.; Robertson, S. Experimental investigations on photoelectric and triboelectric charging of dust. *J. Geophys. Res.* **2001**, *106*, 8343–8356.
- (28) Murtomaa, M.; Räsänen, E.; Rantanen, J.; Bailey, A.; Laine, E.; Mannerman, J. P.; Yliruusi, J. Electrostatic Measurements on a Miniaturized Fluidized Bed. *J. Electrostat.* **2003**, *57*, 91–106.
- (29) Revel, J.; Gatamel, C.; Dodds, J. A.; Taillet, J. Generation of static electricity during fluidisation of polyethylene and its elimination by air ionization. *Powder Technol.* **2003**, *135*, 192–200.
- (30) Krauss, C. E.; Horányi, M.; Robertson, S. Experimental Evidence for Electrostatic Discharge of Dust Near the Surface of Mars. *New J. Phys.* **2003**, *5*, 70.170.9.
- (31) Park, A.-H.; Fan, L.-S. Electrostatic charging phenomenon in gas-liquid-solid flow systems. *Chem. Eng. Sci.* **2007**, *62*, 371–386.
- (32) Yanar, D. K.; Kwetkus, B. A. Electrostatic separation of polymer powders. *J. Electrostat.* **1995**, *35*, 257–266.
- (33) Schonert, K.; Eichas, K.; Niermoller, F. Charge distribution and state of agglomeration after tribocharging fine particulate materials. *Powder Technol.* **1996**, *86*, 41–47.
- (34) Iuga, A.; Calin, L.; Neamtun, V.; Mihalcioiu, A.; Dascalescu, L. Tribocharging of Plastics Granulates in a Fluidized Bed Device. *J. Electrostat.* **2005**, *63*, 937–942.
- (35) Engers, D. A.; Fricke, M. N.; Newman, A. W.; Morris, K. R. Triboelectric charging and dielectric properties of pharmaceutically relevant mixtures. *J. Electrostat.* **2007**, *65*, 571–581.
- (36) Mazumder, M. K.; Ware, R. E.; Yokoyama, T.; Rubin, B. J.; Kamp, D. Measurement of particle size and electrostatic charge distributions on toners using E-SPART analyzer. *IEEE Trans. Ind. Appl.* **1991**, *27*, 611–619.

(37) Trigwell, S.; Grable, N.; Yurteri, C. U.; Sharma, R.; Mazumder, M. K. Effects of Surface Properties on the Tribocharging Characteristics of Polymer Powder as Applied to Industrial Processes. *IEEE Trans. Ind. Appl.* **2003**, *39*, 79–86.

(38) Yurteri, C. U.; Mazumder, M. K.; Grable, N.; Ahuja, G.; Trigwell, S.; Beris, A. S.; Sharma, R.; Sims, R. A. Electrostatic effects on dispersion, transport, and deposition of fine pharmaceutical powders: Development of an experimental method for quantitative analysis. *Part. Sci. Technol.* **2002**, *20*, 59–79.

(39) Schein, L. B.; Czarnecki, W. S.; Christensen, B.; Mu, T.; Galliford, G. Experimental Verification of the Proximity Theory of Toner Adhesion. *J. Imaging Sci. Technol.* **2004**, *48*, 417–425.

(40) Nemeth, E.; Albrecht, V.; Schubert, G.; Simon, F. Polymer triboelectric charging: dependence on thermodynamic surface properties and relative humidity. *J. Electrostat.* **2003**, *58*, 3–16.

(41) Lowell, J.; Rose-Innes, A. C. Contact Electrification. *Adv. Phys.* **1980**, *29*, 947–1023.

*Received for review* March 26, 2008

*Revised manuscript received* May 28, 2008

*Accepted* May 29, 2008

IE8004786